Interpretation of spectral emission around 20 nm region from tungsten ions observed in fusion device plasmas

C Suzuki[1], C S Harte[2], D Kilbane[2], T Kato[1], H A Sakaue[1], I Murakami[1], D Kato[1], K Sato[1], N Tamura[1], S Sudo[1], M Goto[1], R D'Arcy[2], E Sokell[2] and G O'Sullivan[2]

[1] National Institute for Fusion Science, 322-6 Oroshi-cho, Toki 509-5292, Japan
[2] University College Dublin, Belfield, Dublin 4, Ireland

E-mail: csuzuki@nifs.ac.jp

Abstract. We have measured extreme ultraviolet (EUV) spectra from tungsten ions around 20 nm region in plasmas produced in the Large Helical Device at the National Institute for Fusion Science. The spectra after injecting a tungsten pellet into a hydrogen plasma were monitored by a grazing incidence spectrometer. Quasicontinuum spectral feature arising from unresolved transition array (UTA) was observed around 20 nm region in plasmas with temperatures below 1.0 keV. This structure is reasonably considered to be the same one as those observed in another tokamak device or laser produced plasmas under low temperature conditions. Atomic structure calculations have been performed for tungsten ions with open 5p, 5s and 4f subshells (W^{7+}–W^{27+}) to interpret this commonly observed feature around 20 nm. Wavelengths and gA values for these transitions were calculated, and their mean wavelengths and extent were compared with the observations, which suggests that the emission largely arises from $n = 5$–5 transitions in stages lower than W^{27+}.

Submitted to: *J. Phys. B: At. Mol. Opt. Phys.*

1. Introduction

Because tungsten will be used as a plasma facing component in the forthcoming International Thermonuclear Experimental Reactor (ITER), studies on the behavior of tungsten in existing fusion research devices are already underway at a number of major locations worldwide [1]. For example, tungsten erosion rates and the impact of an all tungsten divertor are being studied at Joint European Torus (JET), while interior regions of the ASDEX Upgrade tokamak have been coated with tungsten and an extensive program of study has been ongoing for more than the past ten years on the effects of tungsten impurities on the plasma dynamics [2, 3, 4, 5].

At the plasma temperatures typically attained in a fusion device, tungsten ions will not be fully stripped leading to intense emission in the extreme ultraviolet (EUV) and soft X-ray spectral regions. In all reported work to date [6], it was found that tungsten ions radiate very strongly at 4–7 nm range where a structured quasicontinuum overlaid by a few strong lines was observed. More recently the similar spectra from tungsten ions following pellet injection have been reported in the Large Helical Device (LHD) at the National Institute for Fusion Science (NIFS) [7, 8]. The strong lines were shown to primarily originate from 4d–4f lines in the spectra of Ag-, Pd-, and Rh-like ions (W^{27+}–W^{29+}) [9, 10, 11]. Recent studies in an electron beam ion trap (EBIT) have shown conclusively that $n = 4$–4 transitions in spectra from ions with 4f, 4d and 4p electrons in their outermost subshell emit intensely in the 4–7 nm region [12]. Because of the complexity of the configurations in stages with open 4d and 4f subshells this emission essentially takes the form of quasicontinuum.

Though lower ion stages with 4f, 5s and 5p electrons in their outermost subshells would be important in edge region of the ITER plasma, information on these ions is still insufficient. Indeed, a comprehensive review of the available data for tungsten spectral lines in all ion stages has recently been published by Kramida and Shirai [13], which points out the lack of any definitive spectral data for W^{8+}–W^{26+} inclusive. The spectra for these ions are greatly complicated by the crossings of the 4f and 5p binding energies near W^{6+} and the 5s and 4f near W^{16+} [14]. From studies of laser produced plasmas it was found that the emission from a tungsten plasma, known to contain ions up to W^{15+}, produced broad-band EUV continuum radiation overlaid with very few lines throughout the 3–20 nm spectral region [15, 16, 17]. The only discrete lines observed were from W^{5+} and W^{6+} spectra [18, 19].

In the present work we concentrate on the interpretation of EUV spectra recorded around 20 nm region, obtained in tungsten injection experiments in the LHD under low temperature conditions, where large contributions of charged states lower than Ag-like W^{27+} are expected. The measured spectral feature is considered to be the same one as those measured in ASDEX Upgrade tokamak [5] and the laser produced tungsten plasmas [15, 16, 17]. Nevertheless, the theoretical analysis of these observed structure, which is considered to be from low charged states, have not yet been done. Therefore, in this study, theoretical calculations of gA value distribution have been carried out with

the Hartree Fock with configuration interaction suite of codes written by Cowan [20] to establish the region of the emission and to give an insight to the observed spectra.

2. Experimental observations

LHD is one of the largest devices for magnetically confined fusion research equipped with several numbers of superconducting helical and poloidal coils [21]. The essential details of the experimental setup used in the LHD have already been described elsewhere [22]. A small amount of tungsten was injected by a solid pellet into the low density background hydrogen plasma. The EUV spectra were recorded by a 2 m Schwob Fraenkel grazing incidence spectrometer [24].

Figure 1 shows a survey spectrum around 20 nm measured by a low resoluion grating (133.6 mm^{-1}) in a plasma with an injection of a tungsten pellet ablated in the low temperature edge region below 1 keV. In this discharge, the pellet was composed of a cylindrical tungsten core (0.4 mm diameter and 0.7mm height) surrounded by a graphite shell (1.2 mm diameter and 1.2 height). As shown, the spectral feature just after the pellet injection shows quasicontinum structure in 16–22 nm which has a peak around 18 nm and decreased intensity towards longer wavelength. The present data are comparable to the result from ASDEX Upgrade [5] which shows a broader structure in the 15–25 nm region just after a laser blow off of tungsten, which essentially appears under the plasma temperature below 1.3 keV. On the other hand, Carroll and co-workers observed spectra from laser produced plasmas with solid tungsten targets in the 4–10 nm and 7–20 nm ranges independently by two different grazing incidence spectrographs, and the intensity increased in 12–20 nm, while the structure in 4–7 nm region was absent under the condition that the maximum ion stage would be close to W^{20+} [15, 16, 17].

Figure 2 explains the fact that this spectral feature around 20 nm only appear under the condition of relatively lower electron temperature, and arises from charged states lower than W^{27+}. Time sequences of stored energy (W_p), central electron temperature ($T_e(0)$) and the observed EUV spectra around 21 nm and 5 nm are summarized in figure 2 for two different plasma shots with tungsten pellet injection. In this experiment, a pellet system called tracer encapsulated solid pellet (TESPEL) [23] was used. The neutral beam injection (NBI) heating power was about 11 MW in both shots. The plasma was stably maintained after the pellet injection in the shot (a) #97387 (left hand side of figure 2), while it underwent a radiating collapse in the shot (b) #97386 (right hand side of figure 2). In this experiment, we have chosen 19–23 nm wavelength region primarily, and 4.2–7 nm region was measured at the same time for monitoring the well known strong UTA emission of $n = 4$–4 transition with a grating of 600 mm^{-1} groove density. The integration time of the detector was 200 ms. As shown, in the case of the stably sustained plasma (#97387), only a very weak continuous feature superposed on intrinsic impurity lines are observed in the spectra around 20 nm after the TESPEL injection and no drop of the central electron temperature is observed, while the clear UTA structure around 5 nm from tungsten ions is observed together with clear peaks

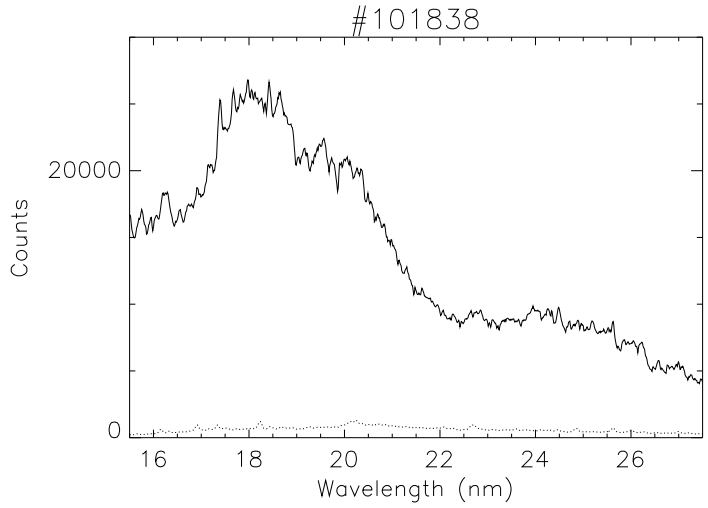

Figure 1. Low resolution spectrum around 20 nm measured in the LHD plasma with a tugsten pellet injection. The spectra before and after the injection are shown in the figure by a solid and dotted lines, respectively.

of Ag-like W^{27+} and Pd-like W^{28+} indicated by arrows [3, 9, 11]. On the other hand, quasicontinuum feature around 20 nm strongly observed in the case of the radiation collapse (#97386), during which the central electron temperature decreased from 1.8 keV to zero at 4.9 s, and the peaks of W^{27+} and W^{28+} almost disappeared in the spectrum around 5 nm. Therefore the structure around 20 nm shown in figure 2 is reasonably considered to be generated by charged states lower than W^{27+}. These experimental results common in different devices indicate the presence of quasicontinuum structure in this wavelength range from relatively low charged tungsten ions (open 4f subshell or lower).

3. Results of calculation

As shown in section 2, the quasicontinuum structure around 20 nm region is considerd to be predominantly emitted from charged states lower than W^{27+}. Sugar and Kaufman identified resonance lines of W^{6+} for 5p–5d transitions at 21.6219, 26.1387 and 31.3573 nm, and for 4f–5d transitions at 28.9526, 29.4376 and 30.2272 nm [19]. However, no difinitive experimental data are available for W^{7+}–W^{26+} [13]. It was also shown in our earlier calculations that 4f–5d transitions in W^{14+} and W^{15+} gave rise to arrays in the 11–13 nm region, and move towards shorter wavelength with increasing charge eventually ending with the Ag-like W^{27+} near 4.4 nm [8]. Hence it is suggested that for the 4f–5d transitions to contribute significantly to the 20 nm structure, the plasmas would need to contain sizeable contributions of W^{7+}–W^{13+}. Nevertheless, in this study, we decided to calculate the positions of $n = 5$–5 transitions in W^{7+}–W^{27+} because wavelengths of $\Delta n = 0$ transitions tend to move more slowly with increasing ionisation and more largely

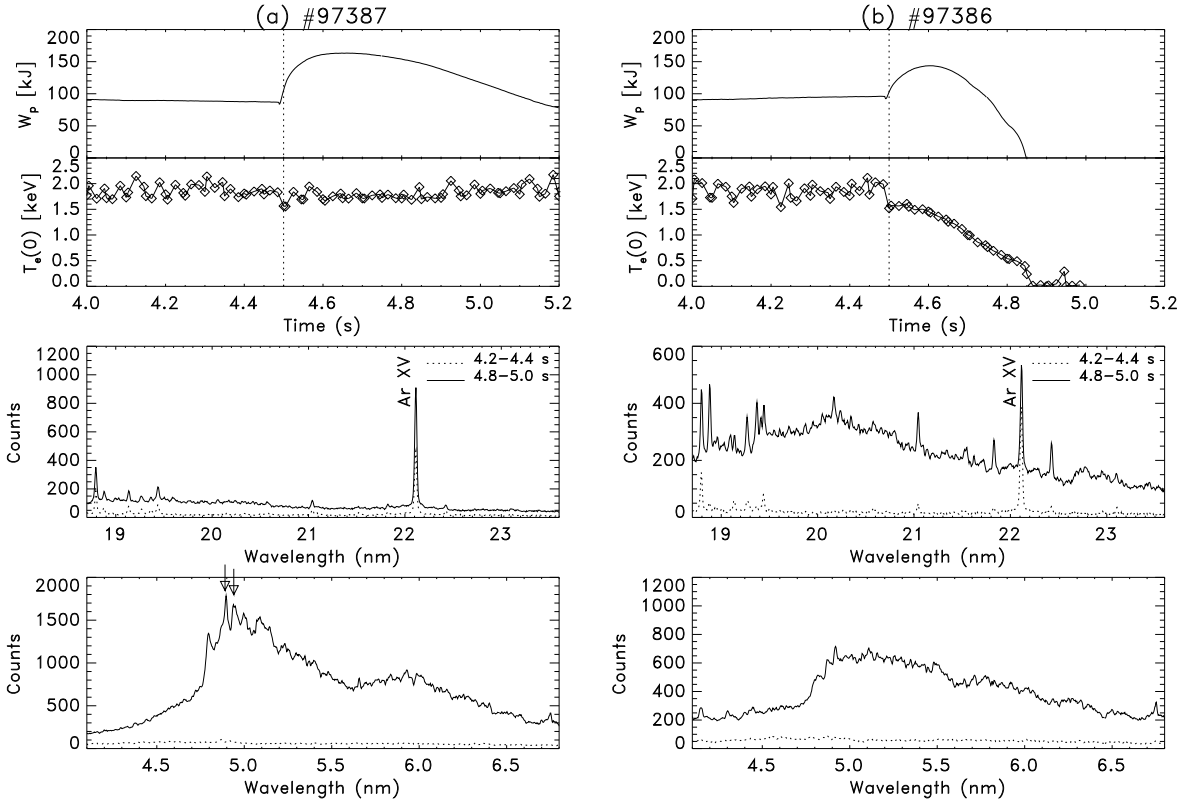

Figure 2. Summary of the temporal evolutions of the discharges and the observed EUV spectra around 21 nm and 5 nm in two different plasma shots with tungsten TESPEL injection at 4.5 s in LHD. Time sequences of stored energy (W_p) and central electron temperature ($T_e(0)$) are displayed. The neutral beam injection (NBI) heating power was about 11 MW in both shots. The plasma was stably maintained after the TESPEL injection in the shot (a) #97387, while it underwent a radiating collapse in the shot (b) #97386. The two peaks near 4.8 nm indicated by arrows in figure (a) are due to Ag-like W^{27+} and Pd-like W^{28+}.

contribute to the observed quasicontinuum structure.

In order to simulate the emission from the contributing ions, calculations were performed with the Hartree Fock with configuration interaction suite of codes written by Cowan [20]. The Slater Condon parameters were scaled to 85% of their ab initio values while the spin orbit integrals were unchanged, a prescription that gave good agreement between theory and observation in our earlier work [8].

3.1. 5p–5d transitions for open 5p/4f subshell ions (W^{7+}–W^{11+})

Subshells from 1s to 4d and 5s are closed, and 5p and/or 4f subshells are open in the ground configurations of W^{7+}–W^{11+} [13]. Therefore we have carried out calculations of 5p–5d transitions for these ion stages. Single configuration average energies for W^{7+} and W^{8+} are listed in table 1. In W^{7+} the $4f^{13}5s^25p^6\ {}^2F^{\circ}_{7/2}$ is predicted to

Table 1. An extracted table of single configuration average energies for tugsten ions (W^{7+}, W^{8+}, W^{12+},W^{13+},W^{17+}) calculated by Cowan code in this study.

Ion Stage	Odd Configuration	E_{av} (eV)	Even Configuration	E_{av} (eV)
W^{7+}	$4f^{13}5s^25p^6$	0	$4f^{14}5s5p^6$	46.73
	$4f^{14}5s^25p^5$	4.09		
W^{8+}	$4f^{13}5s5p^6$	44.38	$4f^{12}5s^25p^6$	4.37
	$4f^{14}5s5p^5$	43.25	$4f^{13}5s^25p^5$	0
			$4f^{14}5s^25p^4$	1.27
			$4f^{14}5p^6$	89.55
W^{12+}	$4f^{12}5s5p^3$	73.02	$4f^{11}5s^25p^3$	53.27
	$4f^{13}5s5p^2$	52.96	$4f^{12}5s^25p^2$	29.31
	$4f^{14}5s5p$	38.92	$4f^{13}5s^25p$	11.67
			$4f^{14}5s^2$	0
W^{13+}	$4f^{10}5s^25p^3$	83.56	$4f^{11}5s5p^3$	94.38
	$4f^{11}5s^25p^2$	49.11	$4f^{12}5s5p^2$	64.17
	$4f^{12}5s^25p$	21.35	$4f^{13}5s5p$	40.41
	$4f^{13}5s^2$	0	$4f^{14}5s$	22.74
W^{17+}	$4f^75s^25p^2$	163.37	$4f^75s5p^3$	214.73
	$4f^95p^2$	120.17	$4f^85s5p^2$	137.87
	$4f^85s^25p$	89.08	$4f^95s5p$	68.98
	$4f^{10}5p$	56.40	$4f^{10}5s$	7.74
	$4f^95s^2$	22.72		
	$4f^{11}$	0		

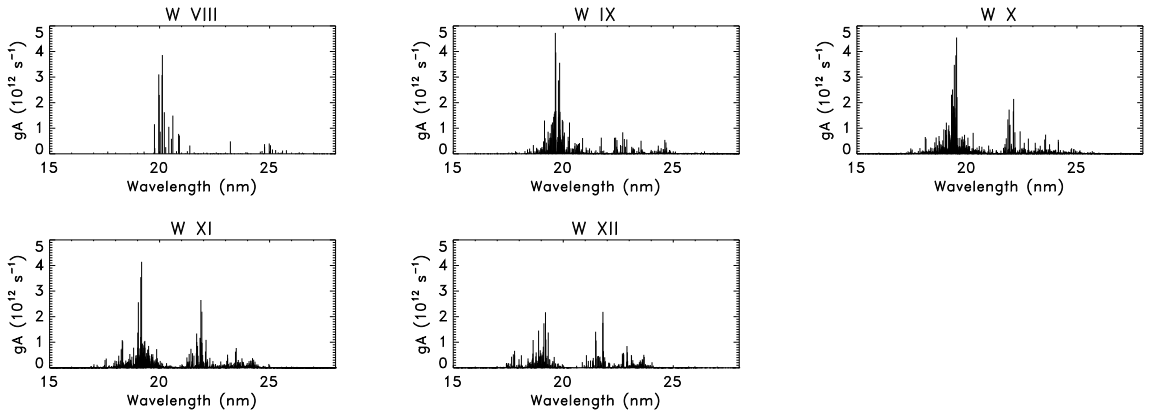

Figure 3. Calculated positions and gA values resulting from 5p–5d transitions in W^{7+}–W^{11+} (W VIII–W XII) corresponding to $4f^{14}5s^25p^n$ + $4f^{13}5s^25p^{n+1}$–$4f^{14}5s^25p^{n-1}5d$ + $4f^{13}5s^25p^n5d$ (n = 1–5).

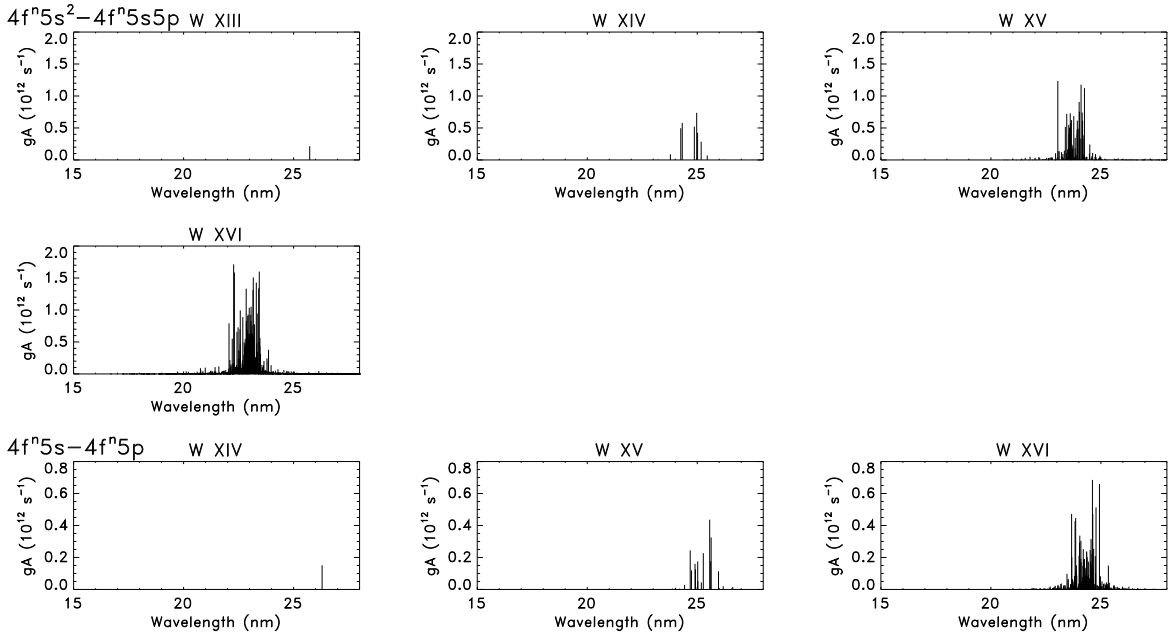

Figure 4. Calculated positions and gA values of 5s–5p$_{1/2}$ transitions in W^{12+}–W^{15+} (W XIII–W XVI). The upper set correspond to $4f^n5s^2$–$4f^n5s5p$ (n = 11–14), and the lower set to $4f^n5s$–$4f^n5p$ (n = 12–14).

lie below the $4f^{14}5s^25p^5\ ^2P^\circ_{3/2}$ by approximately 0.1 eV which is lower than the spin orbit splitting of either configuration. Therefore we calculated $4f^{14}5s^25p^5$+$4f^{13}5s^25p^6$–$4f^{14}5s^25p^45d$+$4f^{13}5s^25p^55d$ transitions with configuration interaction (CI) for this spectrum. For W^{8+} we have three competing configurations: $4f^{14}5s^25p^4$, $4f^{13}5s^25p^5$ and $4f^{12}5s^25p^6$; also CI becomes possible here. Rather than tackling the full CI calculation we limited it to $4f^{14}5s^25p^4$ + $4f^{13}5s^25p^5$– $4f^{14}5s^25p^35d$ + $4f^{13}5s^25p^45d$ as calculations for the 5p–5d transitions with increasing ion stage introduce an additional configuration in successive ions associated with the 5p removal and the calculation becomes impossible due to memory limitations. Moreover the transitions from higher configurations will overlap those from the lower configurations and the primary aim here is to establish the region of the emission, as the gA value distribution will not fully reproduce the spectral shape since it does not take population mechanisms into account. Thus for the remaining spectra, calculations were limited to the transition $4f^{14}5s^25p^n$ + $4f^{13}5s^25p^{n+1}$–$4f^{14}5s^25p^{n-1}5d$ + $4f^{13}5s^25p^n5d$ (n = 1–5) for W^{7+}–W^{11+}. The positions of these arrays are shown in figure 3. It is seen in this figure that the bulk of the emission is clustered in two wavelength regions, 18–20 and 21–24 nm and could indeed contribute to the stronger feature seen in the experimental spectra.

3.2. 5s–5p transitions for open 5s/4f subshell ions (W^{12+}-W^{26+})

Single configuration average energies for W^{12+} and W^{13+} are summarized in table 1. The 5p subshell empties at W^{12+} resulting in a simple $4f^{14}5s^2$ ground state, and the

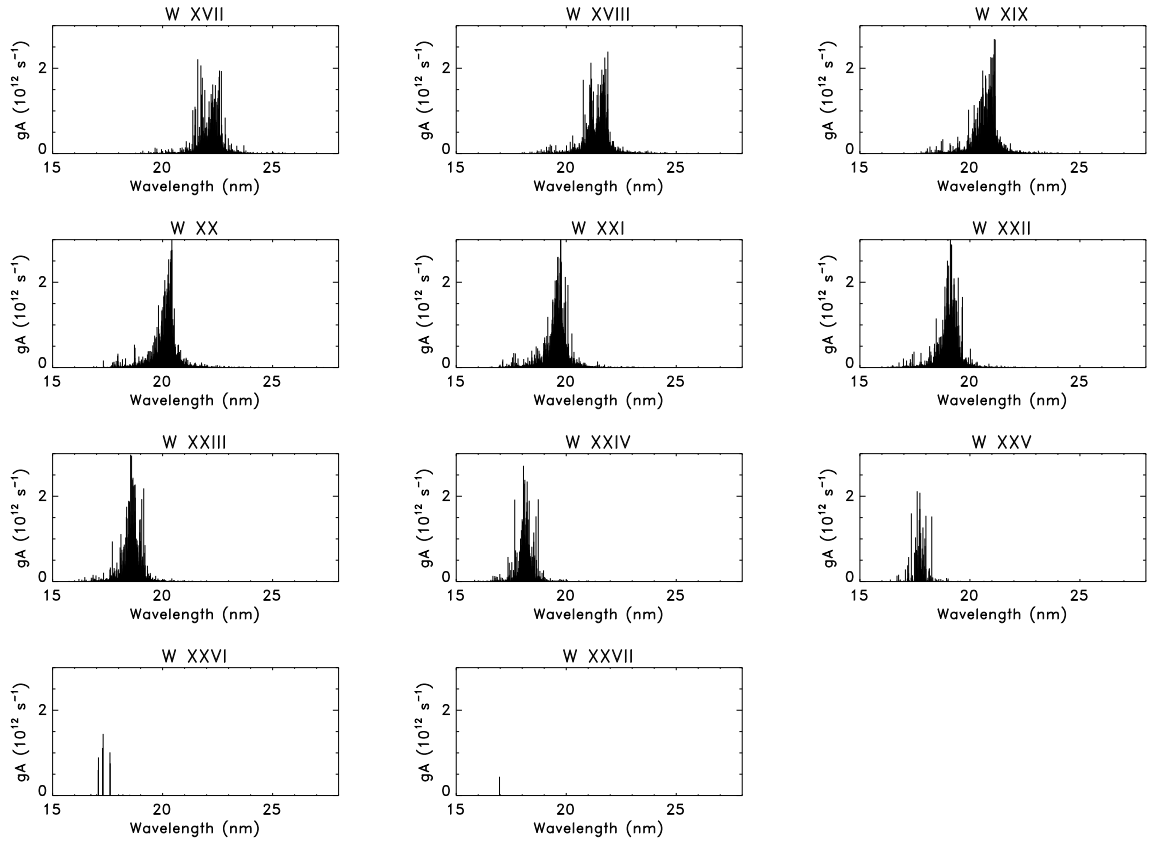

Figure 5. Calculated positions of 5s–5p$_{1/2}$ transitions in W^{16+}–W^{26+} (W XVII–W XXVII) corresponding to $4f^n$+$4f^{n-2}5s^2$–$4f^{n-2}5s5p$ (n = 2–12).

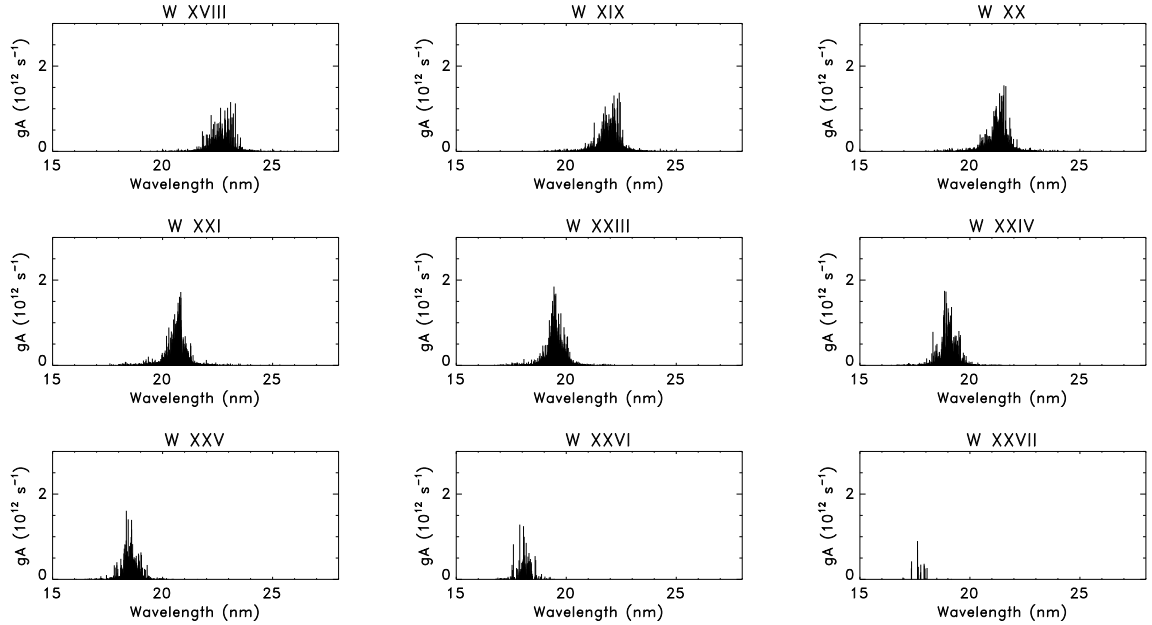

Figure 6. Calculated positions of 5s–5p$_{1/2}$ transitions in W^{16+}–W^{26+} (W XVII–W XXVII) corresponding to $4f^{n-1}5s$–$4f^{n-1}5p$ (n = 2–12).

anticipated position of the $^1S_0$–$^1P_1$ line of $4f^{14}5s5p$–$4f^{14}5s^2$ is 25.73 nm. However competition from transitions involving the $4f^{13}5s^25p$ and other low excited configurations of the same parity with differing 4f and 5p occupancy ($4f^{14-n}5s^25p^n$, n = 1–6, total calculated energy spread of 195.85 eV) will reduce the observed intensity because the 4f and 5s binding energies are so close (see table 1).

In W^{13+} the ground state configuration is the odd parity $4f^{13}5s^2$ and the even parity $4f^{14}5s$ is calculated to lie some 23 eV away as shown in table 1. Though an observation of the $4f^{14}5s\ ^2S_{1/2}$–$4f^{14}5p\ ^2P_{1/2}$ lines have been reported in an electron beam ion trap [25], such lines are unlikely to appear in low density fusion type plasmas which tend to be dominated by resonance transitions to the ground configuration [26, 27]. The lowest odd parity excited configuration, $4f^{12}5s^25p$, begins at 10 eV away but as its centre of gravity ($E_{\rm av}$) is 21.35 away, we chose to ignore it as it will have limited CI effects on the lower configuration and we calculated the 5s–5p transitions involving the $4f^{13}5s^2$ and $4f^{14}5s$ only. Similarly, we calculated 5s–5p transitions for $4f^{12}5s^2$ and $4f^{13}5s$ in W^{14+}; for $4f^{11}5s^2$ and $4f^{12}5s$ in W^{15+}, in which the results are shown in figure 4. Though the spectra form two tight stronger and weaker groupings at 25 nm and 40 nm corresponding to $5s_{1/2}$–$5p_{1/2}$ and $5s_{1/2}$–$5p_{3/2}$ excitations, respectively, only the former component is shown in figure 4.

In W^{16+} the ground configuration is $4f^{11}5s$ and the first excited state is $4f^{10}5s^2$. In W^{17+}–W^{26+}, the ground state becomes $4f^n$ (n = 2–11) and no n = 5 electrons as shown in table 1 for W^{17+}. However, we calculated $4f^n$+$4f^95s^2$–$4f^{n-2}5s5p$ as well as $4f^{n-1}5s$–$4f^{n-1}5p$ for all stages up to W^{26+} by considering CI effects, and the results of these calculations are given in figure 5 and 6 for odd/even lower levels, where we have concentrated on the stronger features arising from $5s_{1/2}$–$5p_{1/2}$ excitation only. The $5s_{1/2}$–$5p_{3/2}$ excitation gives rise to a weak array that lies at 40 nm in W^{14+} and moves to 31 nm in W^{26+} (not shown in the figures).

At the higher ionisation end of this sequence, the overall spread in energies is quite large and since no significant emission is anticipated from other than resonance transitions to the ground state we expect a negligible contribution from these configurations. Nevertheless since optically allowed transitions between these configurations and the lowest $4f^n$ are impossible, we may have some contribution from 5s–5p transitions in these stages in the plasmas of figures 1 and 2 as well. Note that the $5s$–$5p_{1/2}$ transitions extend from 17–25 nm and can thus make a sizable contribution to the 20 nm structure.

3.3. Other n = 5–5 transitions for W^{25+}–W^{27+}

In earlier experiments on Sn and Xe injection in the LHD, it was noted that for the majority of ion stages, only resonance transitions to the ground configuration were observed but a notable exception in each case was provided by Cu-like Sn and Xe ions [22, 27, 28]. Cu-like ions have a single 4s electron outside a closed n = 3 shell. In the present case, Ag-like W^{27+} has a single 4f electron outside a closed 4d subshell. In

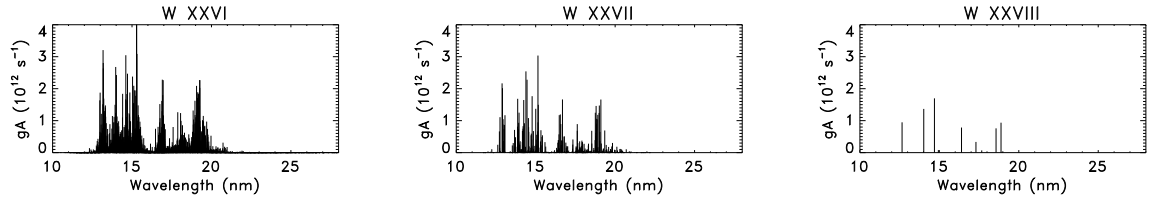

Figure 7. Calculated positions of n = 5–5 transitions in W^{25+}–W^{27+} (W XXVI–W XXVIII) corresponding to $4f^n5s$ + $4f^n5d$ + $4f^n5g$ – $4f^n5p$ +$4f^n5f$ (n = 0–2).

many plasmas, the spectra are dominated by closed shell (rare-gas like) or single electron outside closed shell ions (formed by recombination in the former) because of the large increase in excitation energy needed to remove an electron from the next shell. While the jump in excitation energy needed to remove a 4d electron is low by comparison, nevertheless, the n = 4–4 spectrum of tungsten ions from most fusion device plasmas contains very intense line emission from the $4d^{10}4f$–$4d^94f^2$.

Based on this observation, the positions of the excited $4d^{10}5s$–$4d^{10}5p$, $4d^{10}5p$–$4d^{10}5d$, $4d^{10}5d$–$4d^{10}5f$ and $4d^{10}5f$–$4d^{10}5g$ in Ag-like W^{27+} were calculated with considering CI effects and the results are shown in figure 7. Note that these lines all lie in the 12–20 nm region and the strongest $^2P_{1/2}$–$^2D_{3/2}$, $^2D_{3/2}$–$^2F_{5/2}$ and $^2D_{5/2}$–$^2F_{7/2}$ lie in the 12–15 nm region. To further show the accumulation of possible n = 5–5 transitions in the 20 nm region we calculated the positions of $4f^n5s$ + $4f^n5d$ + $4f^n5g$ – $4f^n5p$ +$4f^n5f$ (n = 0–2) in W^{25+}–W^{27+} as shown in figure 7.

Figure 8 summarizes the calculations for the n = 5–5 transitions in a range of tungsten spectra in this study in terms of ion charge dependence of mean position and array widths indicated by vertical bars.

4. Conclusion

We have measured quasicontinuum spectral feature around 20 nm region arising from UTA of tungsten ions in plasmas produced in the LHD under low temperature conditions below 1.0 keV, similar to the one obseved in ASDEX-Upgrade tokamak. Atomic structure calculations for W^{7+}–W^{27+} shows that the UTA observed in the 20 nm region in both devices result primarily from n = 5–5 transitions. Since small differences in spectral feature between them may be explained by the differences in population of the emitting ions, evaluation of the detailed ion distribution is required to make a detailed comparison. Nevertheless the LHD spectrum could be explained by a strong contribution from 5s–5p transitions in ion stages from W^{17+}–W^{23+}, while the spectra in ASDEX-Upgrade are better explained by allowing for 5p–5d transitions in lower stages also.

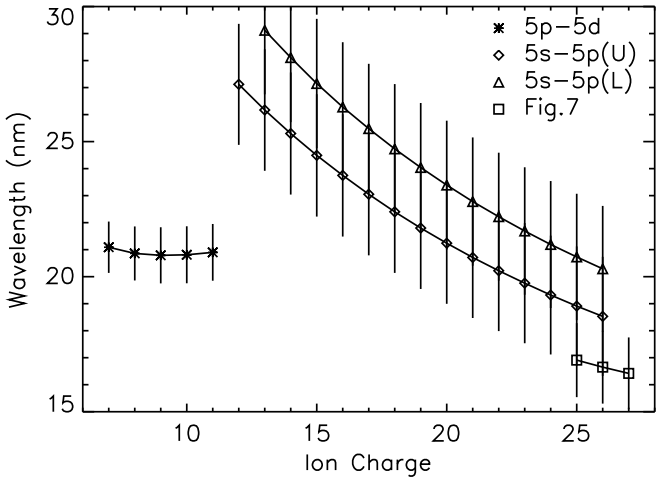

Figure 8. Ion charge dependence of mean position and array widths (indicated by vertical bars) for the $n = 5$–5 transitions in a range of tungsten spectra calculated in this study.

Acknowledgments

The authors acknowledge the LHD experiment group for their assistance. This work was supported by Science Foundation Ireland under Research Grant Number 08-RFP-1100. ES acknowledges support from the Japan Society for the Promotion of Science.

References

[1] Neu R *et al* 2007 *Phys. Scr.* **T128** 150
[2] Neu R, Fournier K B, Schlög D and Rice J 1997 *J. Phys. B: At. Mol. Opt. Phys.* **30** 5057
[3] Asmussen K, Fournier K B, Laming J M, Neu R, Seely J F, Dux R, Engelhardt W, Fuchs J C and ASDEX Upgrade Team 1998 Nucl. Fusion **38** 967
[4] Pütterich T, Neu R, Biedermann C, Radke R and ASDEX Upgrade Team 2005 *J. Phys. B: At. Mol. Opt. Phys.* **38** 3071
[5] Pütterich T, Neu R, Dux R, Whiteford A D, O'Mullane M G and the ASDEX Upgrade Team 2008 *Plasma Phys. Control. Fusion* **50** 085016
[6] Reader J 2009 *Phys. Scr.* **T134** 014023
[7] Chowdhuri M B, Morita S, Goto M, Nishimura H, Nagai K and Fujioka S 2007 *Plasma Fusion Res.* **2** S1060
[8] Harte C S, Suzuki C, Kato T, Sakaue H A, Kato D, Sato K, Tamura N, Sudo S, D'Arcy R, Sokell E, White J and O'Sullivan G 2010 *J. Phys. B: At. Mol. Opt. Phys.* **43** 205004
[9] Sugar J, Kaufman V and Rowan W L 1993 *J. Opt. Soc. Am. B* **10** 1321
[10] Sugar J, Kaufman V and Rowan W L 1993 *J. Opt. Soc. Am. B* **10** 1977
[11] Sugar J, Kaufman V and Rowan W L 1993 *J. Opt. Soc. Am. B* **10** 799
[12] Radtke R, Biedermann C, Schwob J L, Mandelbaum P and Doron R 2001 *Phys. Rev. A* **64** 012720
[13] Kramida A E and Shirai T 2009 *Atomic Data and Nuclear Data Tables* **95** 305
[14] Kilbane D, Cummings A, McGuinness C, Murphy N and O'Sullivan G 2002 *J. Phys. B: At. Mol. Opt. Phys.* **35** 309

[15] Carroll P K and Kennedy E T 1977 *Phys. Rev. Lett.* **38** 1068
[16] Carroll P K, Kennedy E T and O'Sullivan G 1978 *Opt. Lett.* **2** 72
[17] Carroll P K and O'Sullivan G 1982 *Phys. Rev. A* **25** 275
[18] Sugar J and Kaufman V 1979 *J. Opt. Soc. Am.* **69** 141
[19] Sugar J and Kaufman V 1975 *Phys. Rev. A* **12** 994
[20] Cowan R D 1991 *The Theory of Atomic Structure and Spectra* (Berkeley, CA: University of California Press)
[21] Komori A *et al* 2009 *Nucl. Fusion* **49** 104015
[22] Suzuki C, Kato T, Sakaue H A, Kato D, Sato K, Tamura N, Sudo S, Yamamoto N, Tanuma H, Ohashi H, D'Arcy R and O'Sullivan G 2010 2008 *J. Phys. B: At. Mol. Opt. Phys.* **43** 074027
[23] Sudo S *et al* 2002 *Plasma Phys. Control. Fusion* **44** 129
[24] Schwob J L, Wouters A W and Suckewer S 1987 *Rev. Sci. Instrum.* **58** 1601
[25] Hutton R, Zou Y, Reyna Almandos J, Biedermann C, Radtke R, Greier A and Neu R 2003 *Nucl. Instrum. Methods B* **205** 114
[26] Suzuki C, Kato T, Sato K, Tamura N, Kato D, Sudo S, Yamamoto N, Tanuma H, Ohashi H, Suda S, O'Sullivan G and Sasaki A 2009 *J. Phys. Conf. Ser.* **163** 012019
[27] D'Arcy R, Ohashi H, Suda S, Tanuma H, Fujioka S, Nishimura H, Nishihara K, Suzuki C, Kato T, Koike F, White J and O'Sullivan G 2009 *Phys. Rev. A* **79** 042509
[28] Kato T, Funaba H, Sato K, Kato D, Song M-Y, Yamamoto N, Tanuma H, Ohashi H, Sasaki A, Koike F, Nishihara K, Fahy K and O'Sullivan G 2008 *J. Phys. B: At. Mol. Opt. Phys.* **41** 035703